Biogeosciences Discuss., 11, 6039–6067, 2014
www.biogeosciences-discuss.net/11/6039/2014/
doi:10.5194/bgd-11-6039-2014

Biogeosciences Discussions
Open Access

Reduction of ferrihydrite with adsorbed and coprecipitated organic matter: microbial reduction by *Geobacter bremensis* vs. abiotic reduction by Na-dithionite

K. Eusterhues[1], A. Hädrich[2], J. Neidhardt[1], K. Küsel[2,3], T. F. Keller[4,*], K. D. Jandt[4], and K. U. Totsche[1]

[1]Institut für Geowissenschaften, Friedrich-Schiller-Universität Jena, 07749 Jena, Germany
[2]Institut für Ökologie, Friedrich-Schiller-Universität Jena, 07743 Jena, Germany
[3]German Centre for Integrative Biodiversity Research (iDiv) Halle–Jena–Leipzig, 04103 Leipzig, Germany
[4]Chair of Materials Science, Otto Schott Institute of Materials Research, Faculty of Physics and Astronomy, Friedrich-Schiller-University Jena, 07743 Jena, Germany
[*]now at: Deutsches Elektronen-Synchrotron DESY, 22607 Hamburg, Germany

Received: 20 February 2014 – Accepted: 7 April 2014 – Published: 28 April 2014

Correspondence to: K. Eusterhues (karin.eusterhues@uni-jena.de)

Published by Copernicus Publications on behalf of the European Geosciences Union.

Abstract

Ferrihydrite (Fh) is a widespread poorly crystalline Fe oxide which becomes easily coated by natural organic matter (OM) in the environment. This mineral-bound OM entirely changes the mineral surface properties and therefore the reactivity of the original mineral. Here, we investigated the reactivity of 2-line Fh, Fh with adsorbed OM and Fh coprecipitated with OM towards microbial and abiotic reduction of Fe(III). As a surrogate for dissolved soil OM we used a water extract of a Podzol forest floor. Fh-OM associations with different OM-loadings were reduced either by *Geobacter bremensis* or abiotically by Na-dithionite. Both types of experiments showed decreasing initial Fe reduction rates and decreasing degrees of reduction with increasing amounts of mineral-bound OM. At similar OM-loadings, coprecipitated Fhs were more reactive than Fhs with adsorbed OM. The difference can be explained by the smaller crystal size and poor crystallinity of such coprecipitates. At small OM loadings this led to even faster Fe reduction rates than found for pure Fh. The amount of mineral-bound OM also affected the formation of secondary minerals: goethite was only found after reduction of OM-free Fh and siderite was only detected when Fhs with relatively low amounts of mineral-bound OM were reduced. We conclude that direct contact of *G. bremensis* to the Fe oxide mineral surface was inhibited when blocked by OM. Consequently, mineral-bound OM shall be taken into account besides Fe(II) accumulation as a further widespread mechanism to slow down reductive dissolution.

1 Introduction

Natural Fe oxides are typically nanoparticles and contribute significantly to the total surface area and reactivity of a soil (Karltun et al., 2000; van der Zee et al., 2003; Eusterhues et al., 2005; Regelink et al., 2013). Because of their high reactivity towards dissolved organic matter (OM) (Torn et al., 1997; Kaiser and Zech, 2000) it has to be assumed that Fe oxides are partially or completely covered by OM in natural environ-

BGD
11, 6039–6067, 2014

ments. Such coverage may entirely change the original oxide surface with respect to topography, charge, hydrophobicity and functional group distribution. Besides reactivity with respect to further adsorption, this will influence the aggregation behavior of the oxides, their mobility and solubility.

One of the most frequently found Fe oxides is poorly crystalline ferrihydrite (Fh), which usually forms aggregates of only nanometer sized individual crystals (Jambor and Dutrizac, 1998; Bigham et al., 2002; Cornell and Schwertmann, 2003). Organic matter can become associated with Fh by adsorption or coprecipitation. In contrast to adsorption of OM on pre-existing Fh surfaces, coprecipitation leads to adsorption and occlusion (physical entrapment) of organic molecules in the interstices between the Fh crystals. Additionally, the presence of dissolved OM inhibits Fh growth (Schwertmann et al., 2005; Mikutta et al., 2008; Eusterhues et al., 2008; Cismasu et al., 2011), so that coprecipitated Fhs are assumed to develop smaller crystal sizes and more crystallographic defects. Likewise, their aggregation behavior may be affected. Since Fh is often formed in OM-rich solutions, e.g., in sediments and soils, we assume that coprecipitation is a widespread process in nature. As coprecipitated Fhs differ in many properties from pure Fhs, we suppose that the accessibility and solubility of Fh surfaces as well as the accessibility of the adsorbed/occluded OM towards microorganisms, extracellular enzymes, redox active shuttling compounds or reducing agents may differ from Fhs with purely adsorbed OM.

In the past, dissolved humic acids (HA) from alkaline extracts have been added to microbial experiments to test their influence on ferric iron reduction. It was suggested that they may enhance Fe(III) reduction by electron shuttling (Lovley et al., 1996; Hansel et al., 2004; Jiang and Kappler, 2008; Roden et al., 2010), complexation of Fe(II) (Royer et al., 2002) or complexation and dissolution of Fe(III) (Jones et al., 2009). Amstaetter et al. (2012) and Jiang and Kappler (2008) observed that the concentration of HA or the mineral/HA ratio may control whether HAs increase reduction or not. At certain conditions, Amstaetter et al. (2012) even observed a decrease in Fe(III) reduction due to HA addition. The decrease was explained by an increased aggregation and a therefore re-

BGD
11, 6039–6067, 2014

duced accessibility of the Fe oxide surface for bacteria. The influence of mineral-bound HA or OM on reduction is less well investigated. We are aware of only two articles: Henneberry et al. (2012) coprecipitated Fh with dissolved OM from an agricultural drain and exposed the products to S(−II) and Fe(II). Neither a release of the mineral-associated OM nor a mineral transformation was observed during reduction. Shimizu et al. (2013) studied coprecipitated HA on Fh reduction by *Shewanella putrefaciens* strain CN32. Low C/Fe ratios were reported to decrease the reactivity of the Fh-HA associations toward reduction, whereas an increased reactivity was found at high C/Fe ratios.

Our study aims to enlighten changes in Fh reactivity towards microbial and abiotic Fe(III) reduction caused by mineral-bound OM. A water extract of a Podzol forest floor (FFE) was used as OM and served to represent dissolved soil OM. We produced Fhs with different OM loadings by adsorption and coprecipitation, which were then exposed to microbial reduction by *Geobacter bremensis* and chemical reduction by Na-dithionite. Main objectives were to find out whether mineral-bound OM increases or decreases Fh reactivity and whether coprecipitates differ in reactivity from Fhs with adsorbed OM. The formation of secondary minerals was followed by XRD.

2 Methods

2.1 Materials

All compounds used in this study are reagent grade. For preparation of stock solution and media, 18 MΩ doubly deionized water was used. *Geobacter bremensis* (DSM 12179; Straub and Buchholz-Cleven, 2001) was obtained from the German Resource Centre for Biological Material (DSMZ, Braunschweig).

2.2 Extraction of soil organic matter

A forest floor extract (FFE) was obtained from the Oh and Of layers of a Podzol under spruce close to Freising, Germany. Forest floor samples were air-dried and passed

BGD
11, 6039–6067, 2014

through a 2 mm sieve to remove coarse plant remnants. Aliquots of 150 g soil and 700 mL deionized H_2O were shaken end-over-end for 16 h at room temperature and then centrifuged. The supernatant was pressure-filtered through polyvinylidene fluoride (Durapore; 0.45 µm pore width) membranes, concentrated in low temperature rotary evaporators and freeze-dried. The C and N concentration of the FFE was measured using a CN analyzer (Vario EL, Elementar Analysensysteme, Hanau, Germany). A solid-state ^{13}C NMR spectrum was acquired with a Bruker DSX-200 NMR spectrometer (Bruker BioSpin, Karlsruhe, Germany), applying cross polarization with magic angle spinning (CP MAS) at a spinning frequency of 6.8 kHz and a contact time of 1 ms. A ramped ^{1}H pulse was used during contact time to circumvent spin modulation of Hartmann–Hahn conditions. Pulse delays between 200 and 2000 ms were chosen. A transmission FTIR spectrum was taken (Nicolet iS10, Thermo Fisher Scientific, Dreieich, Germany) on a pellet of 2 mg FFE sample diluted with 200 mg KBr between 4000 and 400 cm^{-1}, accumulating 32 scans at a resolution of 4 cm^{-1}.

2.3 Synthesis of Fh and Fh–OM associations

Two-line Fh was produced by titrating a 0.01 M $Fe(NO_3)_3$ solution with 0.1 M NaOH to pH 5. A series of Fhs with different amounts of adsorbed OM were produced by mixing FFE solutions of different C concentrations with suspensions of freshly precipitated 2-line Fh at pH 5. Coprecipitated Fhs were obtained by dissolving $Fe(NO_3)_3$ in FFE solutions of different concentrations and adding 0.1 M NaOH until a pH of 5 was reached. The solid products were separated by centrifugation and pressure filtration, washed twice with deionized H_2O and freeze-dried. The C concentration of these samples was analyzed with the CN analyzer (Vario EL, Elementar Analysensysteme, Hanau, Germany). The specific surface area of the pure Fh was measured by N_2 gas adsorption (Autosorb1, Quantachrome, Odelzhausen, Germany) and calculated according to the BET-equation from 11 data points in the relative pressure range of 0.05 to 0.3. Prior to the measurements the sample was outgassed for at least 16 h at 343 K in vacuum to remove adsorbed water from the sample surfaces. X-ray photoelectron spectra (XPS)

BGD
11, 6039–6067, 2014

were recorded using a Quantum 2000 (PHI Co., Chanhassen, MN, USA) instrument with a focused monochromatic $Al_{K\alpha}$ source (1486.7 eV) for excitation. For the high resolution spectra, the pass energy was set to 58.70 eV. The C/Fe ratio was determined using the peak areas of the C_{1s} and Fe_{2p} peak, after subtracting a Shirley-type background.

2.4 Microbial reduction experiments

Differences in reducibility of Fh and Fh–OM associations and secondary mineralization were studied in liquid cultures inoculated with *G. bremensis*. A defined freshwater medium based on the *Geobacter* medium ATCC 1957, containing 1.5 g L^{-1} NH_4Cl and 0.1 g L^{-1} KCl was used. After autoclaving and cooling under an N_2/CO_2 (80/20 *v*/*v*) atmosphere, 30 mL L^{-1} of 1 M $NaHCO_3$ (autoclaved, CO_2), 10 mL L^{-1} Wolfe's vitamin solution (ATCC1957), 10 mL L^{-1} modified Wolfe's minerals (ATCC1957) and sodium-acetate (7 mM) as carbon source were added. Unless stated otherwise, added solutions were prepared under anoxic (N_2) conditions and filter sterilized (0.2 µm, PVDF). The final medium had a pH of 6.8. NaH_2PO_4 from the original recipe was not added to avoid interaction of PO_4^{3-} with Fh. The medium (10 mL) was dispensed under an N_2 gas stream into pre-sterilized (6 h 180 °C) 21 mL-culture tubes that contained pre-weighed Fh and Fh–OM associations (40 mM per tube). After tubes were closed with butyl rubber stoppers and capped with aluminium rings, they were flushed again with sterile N_2/CO_2 (80/20 *v*/*v*), applying an overpressure of ~ 100 mbar. Pressure was checked with a needle tensiometer (TensioCheck TC1066, Tensiotechnik). Inoculation of Fh and Fh–OM associations was performed with 4.8 % (*v*/*v*; initial cell density ~ 10^8 mL^{-1}) *G. bremensis* pre-culture grown on phosphate-free medium with sodium-fumarate (50 mM) as electron acceptor and sodium-acetate (20 mM) as electron donor and carbon source. Triplicate samples of all treatments were incubated horizontally (30 °C) in the dark and shaken periodically.

BGD
11, 6039–6067, 2014

For Fe(II) determination, 0.2 mL subsamples were taken anoxically from well shaken culture tubes with a syringe and transferred into 0.5 M HCl for extraction (1 h in the dark). Fe(II) of the extraction solutions was determined using the phenanthroline assay (Tamura et al., 1974). Fe(total) was analyzed via ICP-OES (Spectroflame, Spectro, Kleve, Germany). Solid remnants of the incubation experiments were freeze dried and stored under N_2 until XRD measurements (D8 Advance DaVinci diffractometer by Bruker AXS, Karlsruhe, Germany) were performed using Cu Kα radiation at 40 kV and 40 mA.

2.5 Abiotic reduction experiments with Na-dithionite

Chemical reducibility of Fh and Fh–OM associations was evaluated in abiotic reduction experiments performed after Houben (2003). In short, Fh and Fh–OM associations (ca. 0.1 mmol Fe in Fh) were added to 0.5 L of anoxic (N_2) 0.01 M Na-Dithionite solution buffered with ca. 0.015 M $NaHCO_3$ in a 1 L screw cap bottle. Bottles were closed immediately with a rubber stopper and a metal screw cab, shaken thoroughly and afterwards stirred constantly at room temperature. The solution pH was adjusted to ~ 7 before Fh addition by shortly purging with CO_2 and was stable during the experiment. Periodically, samples of 0.5 mL were taken with N_2 flushed syringes and filtered through 0.2 µm membranes (PVDF) into cuvettes filled with 0.5 mL acetate (to quench the reduction) and ddH_2O (for dilution). The dissolved Fe(II) was measured using the phenantroline method (Tamura et al., 1974).

2.6 Evaluation of reduction rates

Fe(II) formation kinetics were used as analogue for Fe(III) reduction. Apparent initial reaction rates were estimated by fitting linear regression lines to Fe(II)/Fe(total) vs. time for the first data points acquired in microbial and abiotic reduction experiments. The slope of the line represents the initial reaction rate. The degree of dissolution was determined at day 17 for microbial experiments and after 75 min for abiotic experiments.

BGD
11, 6039–6067, 2014

Day 17 for microbial experiments was chosen, because the Fe(II)/Fe(total) of the Fh control at day 52 is much lower than at day 17 and therefore probably wrong. We assume that this is due to unintentional oxidation at the end of the experiment in this sample. The data were fit also to a model proposed first by Christoffersen and Christoffersen (1976) and used successfully by e.g. Postma (1993), Larsen and Postma (2001), Houben (2003), and Roden (2004):

$$m_t/m_0 = [-k(1-\gamma)t + 1]^{1/(1-\gamma)}$$

where m_0 is the initial concentration of Fe(III), m_t the concentration of Fe(II) at time t, k the rate constant, and γ a constant describing the Fe-mineral reactivity as controlled by crystal size, morphology, structure and available reactive surface sites (Postma, 1993; Roden, 2004). While we were successful in modeling the abiotic variants, the model failed to reconstruct the biotic dissolution variants (data not shown). This may point to other processes involved in the biotic dissolution, e.g., a preferential selection of a size fraction of the Fh–OM-associations. However, the comparably poor data quality of the biotic variants does not allow for an in-depth interpretation of this finding.

3 Results and discussion

3.1 Characterization of forest floor extract (FFE) and Fh–OM associations

The FFE for the production of Fh–OM associations was characterized by its C/N ratio, solid state ^{13}C NMR and FTIR (Fig. 1). The concentrations of C and N were found to be 35.1 % and 4.3 %. Organic C in the respective chemical shift regions of the NMR spectrum was quantified to 13 % of TOC alkyl C (0–45 ppm), 51 % of TOC O-alkyl C (45–110 ppm), 24 % of TOC aryl C (110–160 ppm), and 13 % of TOC carbonyl C (160–220 ppm). In comparison to the material used for previous adsorption and coprecipitation studies (Eusterhues et al., 2008, 2011, 2014) this material had a higher content in aromatic groups and carbonyl C (ester, carboxyl or amide groups), but a lower

BGD
11, 6039–6067, 2014

content of carbohydrates. The FTIR spectrum (band assignment according to Abdulla et al., 2010) shows strong peaks at 1722 cm^{-1} (C=O of COOH), 1622 cm^{-1} (complexed COO^-) and at 1148, 1089, and 1041 cm^{-1} (C-O in carbohydrates). Very sharp signals at 1384 and 825 cm^{-1} are caused by NO_3^-, and show that only part of the N can belong to amides. Additional smaller signals can be identified using the second derivative of the spectrum: the signal at 1783 cm^{-1} points to the C=O stretching of γ-lactones, signals at 1547 and 1268 cm^{-1} can be explained by amide II and amide III, signals at 1512 and 1218 cm^{-1} are in accordance with the C=C stretching of aromatic rings and with the asymmetric C-O stretching of aromatic OH. The signal at 965 cm^{-1} belongs to the O-H out of plane bending of carboxylic acids and the band at 660 cm^{-1} to the O-H out of plane bending of carbohydrates.

The FFE of this study was taken at the same site as the material used in the previous experiments. Changes in OM composition might be caused by differences in sampling time. In this study, samples were obtained in February directly after snow melt in contrast to summer for the material of previous experiments.

The adsorption isotherm (Fig. 2a) can be described by a BET model (Ebadi et al., 2009) with a monolayer adsorption capacity of $q_m = 0.52\,mg\,m^{-2}$, an equilibrium constant of adsorption for the first layer of $K_S = 0.9\,L\,mg^{-1}$, and an equilibrium constant of adsorption for further layers of $K_L = 0.0045\,L\,mg^{-1}$. The obtained monolayer loading is in accordance with other adsorption studies involving natural OM adsorption and Fh (Tipping et al., 1981; Kaiser et al., 2007; Eusterhues et al., 2005). Coprecipitation, in contrast, produced considerably larger OM-loadings of $\sim 1.1\,mg\,m^{-2}$. This can be explained either by a larger surface area of coprecipitated Fhs or by the presence of occluded OM in addition to adsorbed OM in coprecipitates. Such a behavior was previously reported for the coprecipitation of lignin, but not for a forest floor extract (Eusterhues et al., 2011).

Three samples of each adsorption and the coprecipitation series were selected for the reduction experiments (Table 1).

BGD
11, 6039–6067, 2014

To find out whether the exposed Fh surface differs between coprecipitated Fhs and Fhs with adsorbed OM, we determined the C/Fe-ratio by XPS (Fig. 2b). The highly surface-sensitive XPS technique provides the chemical composition of typically less than 10 nm of the sample surface (Seah and Dench, 1979). Although coprecipitated Fhs might have occluded a major part of the associated OM inside their aggregates, the XPS C/Fe-ratio was found to be similar for samples with the same C concentration. We therefore assume that the accessibility of the Fh surface for reducing agents or microbial cells is not systematically different in coprecipitates and Fhs with adsorbed OM.

3.2 Microbial Fe(III) reduction by *Geobacter bremensis*

Fe reduction kinetics observed during incubation of Fh–OM associations with *G. bremensis* (Fig. 3) revealed that reaction rates and degree of reduction varied with the amount of mineral associated OM: increasing OM-loadings on Fh led to decreasing initial reaction rates and a decreasing degree of reduction for Fhs with coprecipitated as well as adsorbed OM (Table 1). Also, samples of the coprecipitation series were more reactive toward reduction than samples of the adsorption series, when comparing samples with comparable OM contents. For example, in case of AFhA, the sample with the smallest amount of adsorbed OM (44 $mg\,g^{-1}$ C), the initial reaction rate was smaller (0.0017 min^{-1}) than that of the OM-free control Fh (0.0020 min^{-1}) while the degree of dissolution at day 17 was similar (64 %) to that of the control Fh (63 %). In case of CFhA, the Fh sample with the smallest amount of coprecipitated OM (44 $mg\,g^{-1}$ C), initial reaction rate (0.0021 min^{-1}) and degree of dissolution (82 %) were even larger than for the control Fh.

We conclude that the mineral-bound OM results in a surface passivation of the Fh surface. The fact that coprecipitates were more easily reduced than Fhs with adsorbed OM may be explained by smaller and more defective individual Fh crystals in coprecipitates (Eusterhues et al., 2008) and a therefore larger specific surface area. A possibly larger available Fh surface in coprecipitates compared to Fh with the same amount of

BGD
11, 6039–6067, 2014

adsorbed OM was ruled out by XPS (Fig. 2). We assume that the effect of a smaller crystal size dominates over the surface passivation effect due to associated OM in case of the fast and extensive reduction of CFhA. A systematically different aggregate structure between Fh with adsorbed OM and coprecipitated Fhs may also have influenced the availability of the mineral surface.

Our microbial reduction results are surprisingly different from experiments performed by Shimizu et al., (2013), who coprecipitated Fh with standard humic acids and monitored reduction by *Shewanella putrefaciens* strain CN-32. Shimizu et al. (2013) found that increasing amounts of coprecipitated HA led to elevated microbial reduction. At high HA loadings (C/Fe = 4.3) reduction rates based on dissolved Fe(II) were faster than that of pure Fh, whereas lower HA loadings (C/Fe < 1.8) resulted in slower reduction rates. Pure Fh was reduced at medium reduction rates. Although aggregate structure, the ability of HA for ligand exchange and systematic changes in surface charge were discussed to influence reduction kinetics, the experiments of Shimizu et al. (2013) are in accordance with the overall assumption that the coprecipitated HA are used by *Shewanella* to transfer electrons from the cell to Fe oxide and advance its electron shuttling process. A threshold amount of Fh-associated HA was assumed to be necessary before electron shuttling is larger than surface passivation by HA blocking surface sites of Fh (Shimizu et al., 2013).

However, the enhancement of electron shuttling might have been especially strong for the experimental conditions chosen by Shimizu et al. (2013), because the content of aromatic groups and quinones is usually much larger in HA than in forest floor extracts as used in this study. Accordingly, Piepenbrock et al. (2014) could show that the electron accepting capacity, i.e. the concentration of redox-active functional groups, of a natural forest floor extract was only half as high as that of the Pahokee Peat HA.

By comparing the two studies, the question arises if differences in electron transfer mechanisms applied by the δ-Proteobacteria *Geobacter* and the γ-Proteobacteria *Shewanella* can explain whether mineral-bound OM increases or decreases the reducibility of Fe oxides. In general, the following electron transfer strategies have been

BGD
11, 6039–6067, 2014

discussed in the literature: (i) direct electron transfer (DET) by either membrane-bound redox-enzymes (Nevin and Lovley, 2000) or bacterial nanowires (Reguera et al., 2005; Gorby et al., 2006; Malvankar et al., 2011) and (ii) mediated electron transfer (MET) using either chelators (Nevin and Lovley, 2002; Kraemer, 2004) or redox shuttling compounds that are produced by the cell itself (Marsili et al., 2008) or are abundant in the extracellular environment (Lovley et al., 1996). *Geobacter* has been found to require direct contact to the mineral surface, but is also discussed to engage nanowires for electron transfer (Malvankar et al., 2012; Boesen and Nielsen, 2013). *Geobacter* species can conserve energy from the transfer of electrons to a variety of extracellular electron acceptors including metals like Mn(IV) and U(VI), but also electrodes and HA. *Shewanella* is long known to not rely on direct contact (Arnold et al., 1990; Caccavo et al., 1997; Lies et al., 2005) and to produce chelating compounds like flavins (von Canstein, 2008). A study of Kotloski and Gralnick (2013) recently showed that flavin electron shuttling but not direct electron transfer or nanowires is the primary mechanism of extracellular electron transfer by *Shewanella oneidensis*.

For *Geobacter* increasing amounts of mineral-bound OM decreased reduction rates and degree of reduction, probably because reactive surface sites of the mineral are blocked by adsorbed OM molecules. Additionally, increasing amounts of OM will increase the negative charge of the particle surface, which may also impede their accessibility for negatively charged microbial cells (Shimizu et al., 2013 and ref. therein). For *Shewanella* species, which use chelating agents and electron shuttles, smaller amounts of adsorbed OM hinder reduction by passivation of reactive surface sites, whereas large amounts of mineral-bound OM (probably involving an increasingly larger number of weaker bonds between OM and mineral) can be used to enhance electron shuttling or chelating of Fe. Interestingly, we did not observe such an increase in reduction rates at very large OM loadings, although also *Geobacter* species are able to reduce extracellular OM. This can either be explained by the lower concentration of redox active groups in natural dissolved OM compared to HA (Piepenbrock et al., 2014) or by species dependent different capabilities.

BGD
11, 6039–6067, 2014

The often only partial reduction of Fe oxides during microbial reduction is explained by surface passivation by adsorption of Fe(II) (Roden and Urrutia, 1999; Liu et al., 2001). Our study similar to Shimizu et al. (2013) shows that mineral-bound OM has to be taken into account as an additional control of Fe(III) reduction. Because dissolved OM is present in almost all natural environments such as lakes, wetlands and soils, the occurrence of mineral-bound OM on Fe oxides is more likely than that of pure Fe oxides surfaces. Since the precipitation of Fh usually takes place from OM-containing solutions, the occurrence of coprecipitates is also more likely than that of Fh with only adsorbed OM. For these coprecipitates, a smaller crystal size and a more defective structure must be considered to result in faster reaction rates than compared to Fhs with similar amounts of adsorbed OM.

Geobacteraceae have been studied intensively and are thought to contribute significantly to Fe(III)-reduction in most soils and sediments (Lovley, 2011 and ref. therein). Therefore we believe the findings of this study might contribute to a better understanding of processes occurring in a wide variety of environments.

3.3 Mineral transformation during microbial reduction

Investigating the solid remnants after 52 days of microbial reduction revealed that the formation of secondary minerals has been affected by the presence of mineral-bound OM (Table 2). Besides salts, such as halite, sal ammoniac and nahcolite, originating from the medium, we detected the neo-formation of goethite (FeOOH) and siderite ($FeCO_3$). Siderite was found after reduction of pure Fh and in samples with rather low amounts of OM (AFhA, CFhA, CFhB), goethite was only found after reduction of the pure Fh. Thus, the formation of siderite was limited to experiments with high reduction rates and high degrees of reduction, where the solubility product of siderite was likely exceeded. The formation of goethite only took place in the absence of OM. This is in accordance with the general observation that goethite formation is hindered by OM (Schwertmann, 1966, 1970) and with the experiments by Henneberry et al. (2012), who reduced Fh–OM coprecipitates by S(−II) and Fe(II) and observed no mineral transfor-

BGD
11, 6039–6067, 2014

mation as well. Goethite formation during reduction is assumed to be catalyzed by Fe(II) atoms which adsorb to the Fe oxide surface (Hansel et al., 2003; Thompson et al., 2006; Yee et al., 2006). Competition of Fe(II) with OM and therefore decreasing amounts of goethite formation had to be expected in our experiments. However, this does not explain that no goethite was formed during the reduction of Fh with small amounts of mineral-bound OM. The low detection limit of XRD (~ 5 %) or a full coverage of Fe(II)-reactive sites on Fh (Shimizu et al., 2013) should be considered. Shimizu et al. (2013) also found goethite only in the control experiments with pure Fh, whereas the reduction of Fh–OM association favored the formation of green rust and magnetite.

3.4 Abiotic reduction by Na-dithionite

During abiotic reduction with Na-dithionite (Fig. 4, Table 1) we observed highest initial reduction rates for the pure Fh and systematically decreasing reduction rates with increasing amounts of mineral-bound OM. Likewise, the degree of reduction after 75 min is generally decreasing with increasing OM. An exception is sample CFhA, for which the dissolved Fe(II) was estimated to be larger than the total Fe, which is not possible. Therefore we did not calculate reduction rate and degree of reduction for this sample. Reduction rates and the degree of reduction again tend to be larger for coprecipitated Fh. Thus, abiotic reduction experiments displayed the same overall picture of the reactivity of the Fh–OM associations as the microbial reduction experiments with *G. bremensis*. However, reduction rates for Na-dithionite are two to three orders of magnitude larger.

The data for abiotic reduction could be well represented by the model by Christoffersen and Christoffersen (1976; Table 1). It is interesting to note that γ the parameter describing particle shape, particle size, reactive site density and particle heterogeneity in this model is increasing with increasing amounts of mineral-bound OM from 1.3 to 2.6 for coprecipitates and from 2.9 to 7.4 for Fhs with adsorbed OM (Table 1). Reduction of pure Fh gave a γ of 2.4. The theoretical value for ideally dissolving isotropic particles is 2/3. Houben (2003) found a γ of 1.5 for reduction of Fh with Na-dithionite;

BGD
11, 6039–6067, 2014

Larsen et al. (2006) reported values between 1 and 2.2 for reduction of aquifer material by ascorbic acid. Roden (2004) observed a γ of 0.7 for synthetic Fh reduced by ascorbic acid and values between 0.8 and 1.8 for natural Fe oxides. Reducing the same material microbially by *Shewanella* led to much higher values of γ of 5.8 to 11.8. Likewise he observed lower degrees of reduction for microbial reduction than for reduction by ascorbic acid. He concluded that the low degrees of reduction as well as the high values for γ during microbial reduction reflect "the inhibitory effect of Fe(II) accumulation on enzymatic electron transfer". However, because we observed high γ values for abiotic reduction (Table 1), we propose that surface passivation by OM leads to a high γ, also.

These results are of interest for technical and analytical applications, aiming at removing natural Fe oxides, e.g., for Fh-rich encrustration of wells, but also regarding the widely used dissolution of total Fe oxides with Na-dithionite to quantify oxidic Fe(III).

3.5 Summary and environmental implications

Mineral-bound soil OM has been shown to decrease the reactivity of Fh toward both microbial reduction by *G. bremensis* and abiotic reduction by Na-dithionite. The reactivity of Fhs with adsorbed OM differed from Fhs which were coprecipitated with OM: at similar OM contents higher initial reaction rates and higher degrees of reduction were observed for coprecipitated Fhs. Their higher reactivity can be explained by the smaller crystal size and higher number of crystal defects due to crystal poisoning by OM during coprecipitation. However, other aspects such as a different composition of the associated OM, a different aggregate structure may also influence reduction kinetics. At low concentrations of coprecipitated OM these effects may be stronger than the surface passivation by the mineral-bound OM and lead to an even faster reduction of coprecipitates than of pure Fh. We therefore propose that, in addition to the accumulation of Fe(II), the OM coverage of Fe oxide surfaces is discussed as a further widespread mechanism to slow down or cease enzymatic reduction.

BGD
11, 6039–6067, 2014

The secondary formation of Fe minerals resulting from microbial reduction was also influenced by the amount of mineral-bound OM. Goethite was only found after reduction of the OM-free Fh and siderite was only detected when Fhs with relatively low amounts of mineral-bound OM were reduced. For e.g. soils, where we assume that an OM covered Fe oxide surface is rather the rule than the exception, we conclude that goethite and siderite formation is less likely than in typical microbial reduction experiments. Growth of new minerals will influence the cycling of Fe as well as of the usually associated nutrients and contaminants, because both goethite and siderite represent thermodynamically more stable sinks for the fixation of Fe(III) and Fe(II) than Fh and display different mineral surfaces.

Comparison to the study of Shimizu et al. (2013) let us assume that the electron transfer mechanism of a microorganism controls whether or not mineral-bound OM decreases or increases microbial reduction. Whereas *Shewanella* may use own redox-active products to enhance electron shuttling, direct contact requiring *Geobacter* may not be able to reach the oxide surface when blocked by OM.

For natural environments inhabited by diverse microbial communities, these results mean that the likely presence of mineral-bound OM on Fe oxide surfaces may increase or decrease Fe reduction, depending on the dominating types of microorganisms. On the other hand, the composition or activity of the Fe reducing microbial community might be regulated by the mean coverage of the Fe oxide surfaces. Systems with low dissolved OM concentrations and low OM loadings on Fe oxides might be favored by microorganisms requiring direct contact for reduction such as *Geobacter*, whereas systems with high dissolved OM concentrations might be ideal for electron shuttle or ligand driven microbial reduction.

4 Conclusions

Fe oxides are recognized as very important mineral phases, which protect their mineral-bound OM against microbial degradation in the long-term. In redoximorphic soils, it

BGD
11, 6039–6067, 2014

will depend on the type of reducing microorganism whether the presence of mineral-bound OM will inhibit dissolution of the carrier mineral and support OM storage at the same time. When direct electron transfer is the main mechanism for microbial Fe(III) reduction, the OM coverage will protect the underlying Fe mineral and promote its own preservation, whereas the opposite must be assumed for soils dominated by microorganisms using electron shuttles or ligands for Fe(III) reduction.

Acknowledgements. Part of this work was financially supported by the priority program SPP 1315 "Biogeochemical Interfaces in Soil" of the Deutsche Forschungsgemeinschaft (DFG). Many thanks to Angelika Kölbl, Markus Steffens and Ingrid Kögel-Knabner (Lehrstuhl für Bodenkunde, Technische Universität München) for NMR-data and to Ralf Wagner (Chair of Materials Science, University of Jena) for XPS measurements. We also highly appreciate help in the laboratory by Katy Pfeiffer, Gundula Rudolph and Christine Götze.

References

Abdulla, H. A. N., Minor, E. C., Dias, R. F., and Hatcher, P. G.: Changes in the compound classes of dissolved organic matter along an estuarine transect: a study using FTIR and C-13 NMR, Geochim. Cosmochim. Ac., 74, 3815–3838, 2010.

Amstaetter, K., Borch, T., and Kappler, A.: Influence of humic acid imposed changes of ferrihydrite aggregation on microbial Fe(III) reduction, Geochim. Cosmochim. Ac., 85, 326–341, 2012.

Arnold, R. G., Hoffmann, M. R., Dichristina, T. J., and Picardal, F. W.: Regulation of dissimilatory Fe(III) reduction activity in *Shewanella-Putrefaciens*, Appl. Environ. Microb., 56, 2811–2817, 1990.

Bigham, J. M., Fitzpatrick, R. W., and Schulze, D. G.: Iron oxides, in: Soil Mineralogy with Environmental Applications, edited by: Dixon, J. B. and Schulze, D. G., SSSA Book Ser. No. 7, Soil Science Society of America, Madison, WI, 2002.

Boesen, T. and Nielsen, L. P.: Molecular Dissection of Bacterial Nanowires, Mbio, e00270-13, doi:10.1128/mBio.00270-13, 2013.

BGD
11, 6039–6067, 2014

Caccavo, F., Schamberger, P. C., Keiding, K., and Nielsen, P. H.: Role of hydrophobicity in adhesion of the dissimilatory Fe(III)-reducing bacterium *Shewanella alga* to amorphous Fe(III) oxide, Appl. Environ. Microb., 63, 3837–3843, 1997.

Christoffersen, J. and Christoffersen, M. R.: Kinetics of dissolution of calcium-sulfate-dihydrate in water, J. Cryst. Growth, 35, 79–88, 1976.

Cismasu, A. C., Michel, F. M., Tcaciuc, A. P., Tyliszczak, T., and Brown, J. G. E.: Composition and structural aspects of naturally occurring ferrihydrite, CR Geosci., 343, 210–218, 2011.

Cornell, R. M. and Schwertmann, U.: The Iron Oxides: Structure, Properties, Reactions, Occurrences and Uses, Wiley-VCH Verlagsgesellschaft, Weinheim, 2003.

Ebadi, A., Mohammadzadeh, J. S. S., and Khudiev, A.: What is the correct form of BET isotherm for modeling liquid phase adsorption? Adsorption, 15, 65–73, 2009.

Eusterhues, K., Rumpel, C., and Kögel-Knabner, I.: Organo-mineral associations in sandy acid forest soils: importance of specific surface area, iron oxides and micropores, Eur. J. Soil Sci., 56, 753–763, 2005.

Eusterhues, K., Wagner, F. E., Häusler, W., Hanzlik, M., Knicker, H., Totsche, K. U., Kögel-Knabner, I., and Schwertmann, U.: Characterization of ferrihydrite–soil organic matter coprecipitates by X-ray diffraction and Mössbauer spectroscopy, Environ. Sci. Technol., 42, 7891–7897, 2008.

Eusterhues, K., Rennert, T., Knicker, H., Kögel-Knabner, I., Totsche, K. U., and Schwertmann, U.: Fractionation of organic matter due to reaction with ferrihydrite: coprecipitation versus adsorption, Environ. Sci. Technol., 45, 527–533, 2011.

Eusterhues, K., Neidhardt, J., Hädrich, A., Küsel, K., and Totsche, K. U.: Biodegradation of ferrihydrite-associated organic matter, Biogeochemistry, available at: http://link.springer.com/article/10.1007/s10533-013-9943-0/fulltext.html, doi:10.1007/s10533-013-9943-0, 2014.

Gorby, Y. A., Yanina, S., McLean, J. S., Rosso, K. M., Moyles, D., Dohnalkova, A., Beveridge, T. J., Chang, I. S., Kim, B. H., Kim, K. S., Culley, D. E., Reed, S. B., Romine, M. F., Saffarini, D. A., Hill, E. A., Shi, L., Elias, D. A., Kennedy, D. W., Pinchuk, G., Watanabe, K., Ishii, S. I., Logan, B., Nealson, K. H., and Fredrickson, J. K.: Electrically conductive bacterial nanowires produced by Shewanella oneidensis strain MR-1 and other microorganisms, P. Natl. Acad. Sci. USA, 103, 11358–11363, 2006.

Hansel, C. M., Benner, S. G., Neiss, J., Dohnalkova, A., Kukkadapu, R. K., and Fendorf, S.: Secondary mineralization pathways induced by dissimilatory iron reduction of ferrihydrite under advective flow, Geochim. Cosmochim. Ac., 67, 2977–2992, 2003.

BGD
11, 6039–6067, 2014

Hansel, C. M., Benner, S. G., Nico, P., and Fendorf, S.: Structural constraints of ferric (hydr)oxides on dissimilatory iron reduction and the fate of Fe(II), Geochim. Cosmochim. Ac., 68, 3217–3229, 2004.
Henneberry, Y. K., Kraus, T. E. C., Nico, P. S., and Horwath, W. R.: Structural stability of coprecipitated natural organic matter and ferric iron under reducing conditions, Org. Geochem., 48, 81–89, 2012.
Houben, G. J.: Iron oxide incrustations in wells. Part 2: Chemical dissolution and modeling, Appl. Geochem., 18, 941–954, 2003.
Jambor, J. L. and Dutrizac, J. E.: Occurrence and constitution of natural and synthetic ferrihydrite, a widespread iron oxyhydroxide, Chem. Rev., 98, 2549–2585, 1998.
Jiang, J. and Kappler, A.: Kinetics of microbial and chemical reduction of humic substances: implications for electron shuttling, Environ. Sci. Technol., 42, 3563–3569, 2008.
Jones, A. M., Collins, R. N., Rose, J., and Waite, T. D.: The effect of silica and natural organic matter on the Fe(II)-catalysed transformation and reactivity of Fe(III) minerals, Geochim. Cosmochim. Ac., 73, 4409–4422, 2009.
Kaiser, K. and Zech, W.: Dissolved organic matter sorption by mineral constituents of subsoil clay fractions, J. Plant Nutr. Soil Sc., 163, 531–535, 2000.
Kaiser, K., Mikutta, R., and Guggenberger, G.: Increased stability of organic matter sorbed to ferrihydrite and goethite on aging, Soil Sci. Soc. Am. J., 71, 711–719, 2007.
Karltun, E., Bain, D. C., Gustafsson, J. P., Mannerkoski, H., Murad, E., Wagner, U., Fraser, A. R., McHardy, W. J., and Starr, M.: Surface reactivity of poorly-ordered minerals in podzol B horizons, Geoderma, 94, 265–288, 2000.
Kotloski, N. J. and Gralnick, J. A.: Flavin electron shuttles dominate extracellular electron transfer by *Shewanella oneidensis*, Mbio, e00553, doi:10.1128/mBio.00553-12, 2013.
Kraemer, S. M.: Iron oxide dissolution and solubility in the presence of siderophores, Aquat. Sci., 66, 3–18, 2004.
Larsen, O. and Postma, D.: Kinetics of reductive bulk dissolution of lepidocrocite, ferrihydrite, and goethite, Geochim. Cosmochim. Ac., 65, 1367–1379, 2001.
Larsen, O., Postma, D., and Jakobsen, R.: The reactivity of iron oxides towards reductive dissolution with ascorbic acid in a shallow sandy aquifer – (Romo, Denmark), Geochim. Cosmochim. Ac., 70, 4827–4835, 2006.
Lies, D. P., Hernandez, M. E., Kappler, A., Mielke, R. E., Gralnick, J. A., and Newman, D. K.: *Shewanella oneidensis* MR-1 uses overlapping pathways for iron reduction at a distance and

BGD
11, 6039–6067, 2014

by direct contact under conditions relevant for biofilms, Appl. Environ. Microb., 71, 4414–4426, 2005.
Liu, C. X., Kota, S., Zachara, J. M., Fredrickson, J. K., and Brinkman, C. K.: Kinetic analysis of the bacterial reduction of goethite, Environ. Sci. Technol., 35, 2482–2490, 2001.
Lovley, D. R., Coates, J. D., BluntHarris, E. L., Phillips, E. J. P., and Woodward, J. C.: Humic substances as electron acceptors for microbial respiration, Nature, 382, 445–448, 1996.
Lovley, D. R., Ueki, T., Zhang, T., Malvankar, N. S., Shrestha, P. M., Flanagan, K. A., Aklujkar, M., Butler, J. E., Giloteaux, L., Rotaru, A.-E., Holmes, D. E., Franks, A. E., Orellana, R., Risso, C., and Nevin, K. P.: *Geobacter*: the microbe electric's physiology, ecology, and practical applications, in: Advances in Microbial Physiology, vol. 59, edited by: Poole, R. K., 2011.
Malvankar, N. S., Vargas, M., Nevin, K. P., Franks, A. E., Leang, C., Kim, B.-C., Inoue, K., Mester, T., Covalla, S. F., Johnson, J. P., Rotello, V. M., Tuominen, M. T., and Lovley, D. R.: Tunable metallic-like conductivity in microbial nanowire networks, Nat. Nanotechnol., 6, 573–579, 2011.
Malvankar, N. S., Tuominen, M. T., and Lovley, D. R.: Comment on "On electrical conductivity of microbial nanowires and biofilms" by Strycharz-Glaven et al. (2011), Energ. Environ. Sci., 5, 6247–6249, 2012.
Marsili, E., Baron, D. B., Shikhare, I. D., Coursolle, D., Gralnick, J. A., and Bond, D. R.: *Shewanella secretes* flavins that mediate extracellular electron transfer, P. Natl. Acad. Sci. USA, 105, 3968–3973, 2008.
Mikutta, C., Mikutta, R., Bonneville, S., Wagner, F., Voegelin, A., Christl, I., and Kretzschmar, R.: Synthetic coprecipitates of exopolysaccharides and ferrihydrite. Part I: Characterization, Geochim. Cosmochim. Ac., 72, 1111–1127, 2008.
Nevin, K. P. and Lovley, D. R.: Lack of production of electron-shuttling compounds or solubilization of Fe(III) during reduction of insoluble Fe(III) oxide by *Geobacter metallireducens*, Appl. Environ. Microb., 66, 2248–2251, 2000.
Nevin, K. P. and Lovley, D. R.: Mechanisms for accessing insoluble Fe(III) oxide during dissimilatory Fe(III) reduction by *Geothrix fermentans*, Appl. Environ. Microb., 68, 2294–2299, 2002.
Piepenbrock, A., Schröder, C., and Kappler, A.: Electron transfer from humic substances to biogenic an abiogenic Fe(III) oxyhydroxide minerals, Environ. Sci. Technol., 48, 1656–1664, 2014.

BGD
11, 6039–6067, 2014

Postma, D.: The reactivity of iron-oxides in sediments – a kinetic approach, Geochim. Cosmochim. Ac., 57, 5027–5034, 1993.
Regelink, I. C., Weng, L., Koopmans, G. F., and Van Riemsdijk, W. H.: Asymmetric flow field-flow fractionation as a new approach to analyse iron-(hydr)oxide nanoparticles in soil extracts, Geoderma, 202, 134–141, 2013.
Reguera, G., McCarthy, K. D., Mehta, T., Nicoll, J. S., Tuominen, M. T., and Lovley, D. R.: Extracellular electron transfer via microbial nanowires, Nature, 435, 1098–1101, 2005.
Roden, E. E.: Analysis of long-term bacterial vs. chemical Fe(III) oxide reduction kinetics, Geochim. Cosmochim. Ac., 68, 3205–3216, 2004.
Roden, E. E. and Urrutia, M. M.: Ferrous iron removal promotes microbial reduction of crystalline iron(III) oxides, Environ. Sci. Technol., 33, 2492–2492, 1999.
Roden, E. E., Kappler, A., Bauer, I., Jiang, J., Paul, A., Stoesser, R., Konishi, H., and Xu, H. F.: Extracellular electron transfer through microbial reduction of solid-phase humic substances, Nat. Geosci., 3, 417–421, 2010.
Royer, R. A., Burgos, W. D., Fisher, A. S., Jeon, B. H., Unz, R. F., and Dempsey, B. A.: Enhancement of hematite bioreduction by natural organic matter, Environ. Sci. Technol., 36, 2897–2904, 2002.
Schwertmann, U.: Inhibitory effect of soil organic matter on crystallization of amorphous ferric hydroxide, Nature, 212, 645–646, 1966.
Schwertmann, U.: Influence of various simple organic anions on formation of goethite and hematite from amorphous ferric hydroxide, Geoderma, 3, 207–214, 1970.
Schwertmann, U., Wagner, F., and Knicker, H.: Ferrihydrite-humic associations: magnetic hyperfine interactions, Soil Sci. Soc. Am. J., 69, 1009–1015, 2005.
Seah, M. P. and Dench, W. A.: Quantitative electron spectroscopy of surfaces: a standard data base for electron inelastic mean free paths in solids, Surf. Interface Anal., 1, 2–11, 1979.
Shimizu, M., Zhou, J., Schroeder, C., Obst, M., Kappler, A., and Borch, T.: Dissimilatory reduction and transformation of ferrihydrite-humic acid coprecipitates, Environ. Sci. Technol., 47, 13375–13384, 2013.
Straub, K. L. and Buchholz-Cleven, B. E. E.: *Geobacter bremensis* sp. nov. and *Geobacter pelophilus* sp. nov., two dissimilatory ferric-iron-reducing bacteria, Int. J. Syst. Evol. Micr., 51, 1805–1808, 2001.

BGD
11, 6039–6067, 2014

Tamura, H., Goto, K., Yotsuyan T., and Nagayama, M.: Spectrophotometric determination of iron(II) with 1,10-phenanthroline in presence of large amounts of iron(III), Talanta, 21, 314–318, 1974.

Thompson, A., Chadwick, O. A., Rancourt, D. G., and Chorover, J.: Iron-oxide crystallinity increases during soil redox oscillations, Geochim. Cosmochim. Ac., 70, 1710–1727, 2006.

Tipping, E.: The adsorption of aquatic humic substances by iron-oxides, Geochim. Cosmochim. Ac., 45, 191–199, 1981.

Torn, M. S., Trumbore, S. E., Chadwick, O. A., Vitousek, P. M., and Hendricks, D. M.: Mineral control of soil organic carbon storage and turnover, Nature, 389, 170–173, 1997.

von Canstein, H., Ogawa, J., Shimizu, S., and Lloyd, J. R.: Secretion of flavins by Shewanella species and their role in extracellular electron transfer, Appl. Environ. Microb., 74, 615–623, 2008.

van der Zee, C., Roberts, D. R., Rancourt, D. G., and Slomp, C. P.: Nanogoethite is the dominant reactive oxyhydroxide phase in lake and marine sediments, Geology, 31, 993–996, 2003.

Yee, N., Shaw, S., Benning, L. G., and Nguyen, T. H.: The rate of ferrihydrite transformation to goethite via the Fe(II) pathway, Am. Mineral., 91, 92–96, 2006.

BGD
11, 6039–6067, 2014

Table 1. Carbon concentration and C/Fe of Fh-OM associations and results of microbial and abiotic reduction experiments.

				Reduction by *Geobacter bremensis*			Reduction by Na-dithionite					
				linear fit			linear fit			C and C		
		C $mg\,g^{-1}$	C/Fe $mol\,mol^{-1}$	k h^{-1}	r^2	degree of dissolution %[a]	k h^{-1}	r^2	degree of dissolution %[b]	k h^{-1}	γ	r^2
control	Fh	–	–	0.0020	0.961	63	5.29	0.998	83	5.79	2.4	0.989
ad-	AFhA	44	0.39	0.0017	0.955	64	1.59	0.895	62	2.26	2.9	0.990
sorbed	AFhB	105	1.04	0.0011	0.965	42	0.72	0.895	30	1.07	7.2	0.991
OM	AFhD	181	2.46	0.0010	0.939	36	0.67	0.811	24	0.60	7.4	0.979
copreci-	CFhA	44	0.41	0.0021	0.950	82	–[c]	–	–	–	–	–
pitated	CFhB	98	1.06	0.0016	0.983	68	1.09	0.975	64	1.32	1.9	0.995
OM	CFhD	182	2.83	0.0014	0.948	41	0.18	0.975	20	0.21	2.6	0.996

[a] Degree of dissolution at day 17.
[b] Degree of dissolution at 75 min.
[c] Please note that for the reduction by Na-dithionite for sample CFhA the dissolved Fe(II) was estimated to be larger than the total Fe, which is not possible. Therefore we did not calculate reduction rate and degree of reduction for this sample.

BGD
11, 6039–6067, 2014

Table 2. Mineral identification by XRD after reduction by *G. bremensis*. Sal ammoniac (NH_4Cl) is abbreviated by "sal", nahcolite ($NaHCO_3$) by "nahc".

		halite	sal	nahc	calcite	siderite	goethite
control	Fh	×	×	×	×	×	×
adsorbed OM	AFhA	×				×	
	AFhB	×	(×)[a]				
	AFhD	×	×				
coprecipitated OM	KFhA	×	×			×	
	KFhB	×	×	×		×	
	KFhD	×	×				

[a] (×) less than 3 peaks identified.

BGD
11, 6039–6067, 2014

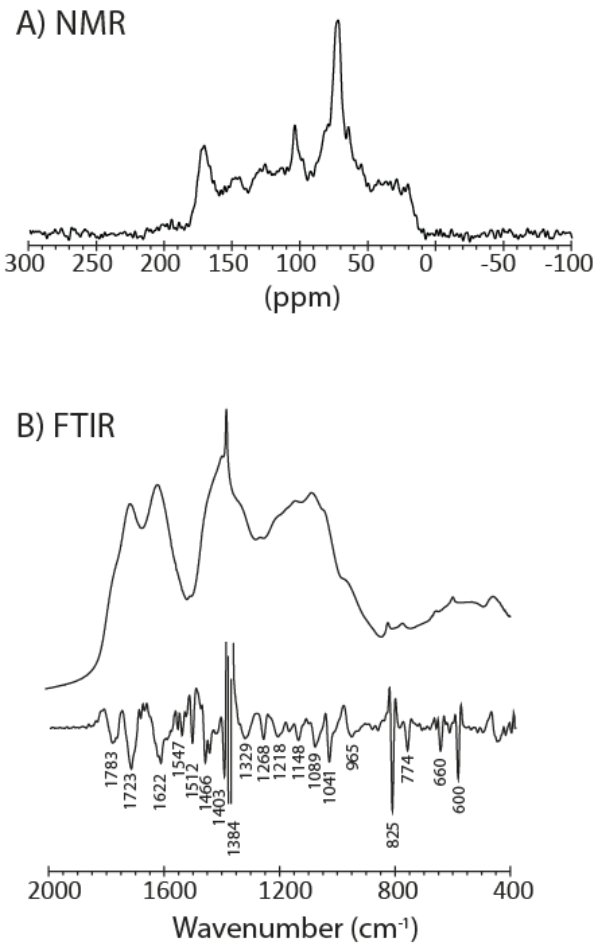

Fig. 1. Characterization of the forest floor extract (FFE): **(A)** ^{13}C CPMAS NMR spectrum, **(B)** FTIR spectrum (top) and second derivative of the FTIR spectrum (bottom).

BGD
11, 6039–6067, 2014

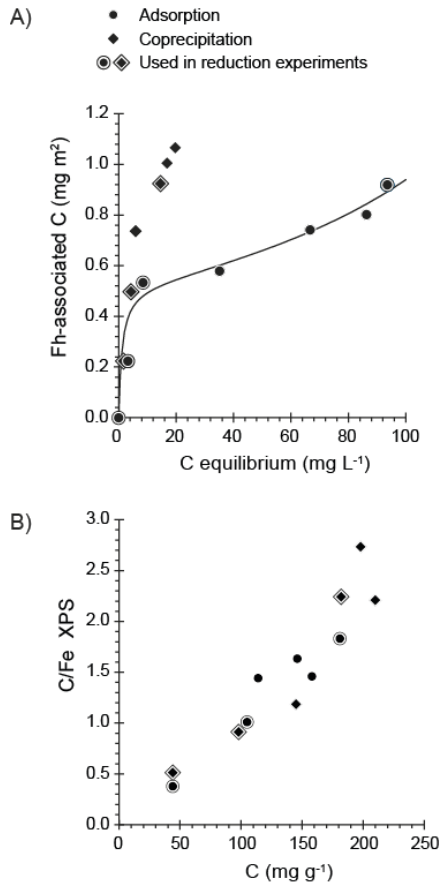

Fig. 2. Organic C loadings on Fh–OM associations normalized to the specific surface area of the control Fh (197 $m^2 g^{-1}$). The line represents a BET-isotherm **(A)**. Comparison between chemical surface and bulk composition: C/Fe ratio as obtained from XPS vs. C concentration of Fh–OM associations **(B)**.

BGD
11, 6039–6067, 2014

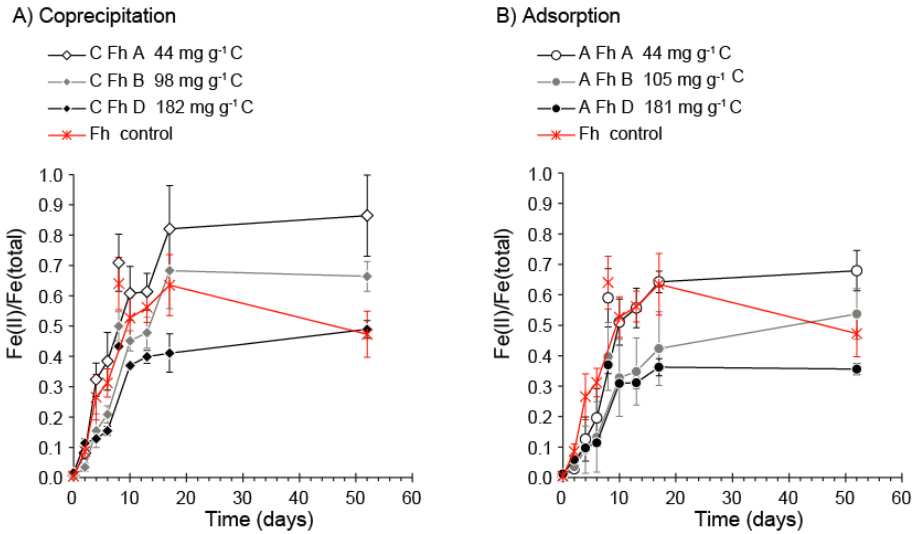

Fig. 3. Microbial reduction of Fh and Fh–OM associations in *Geobacter bremensis* cultures. The Fe(II) production was normalized to the total initial amount of Fe in Fh. Error bars represent standard deviations of triplicate cultures.

BGD
11, 6039–6067, 2014

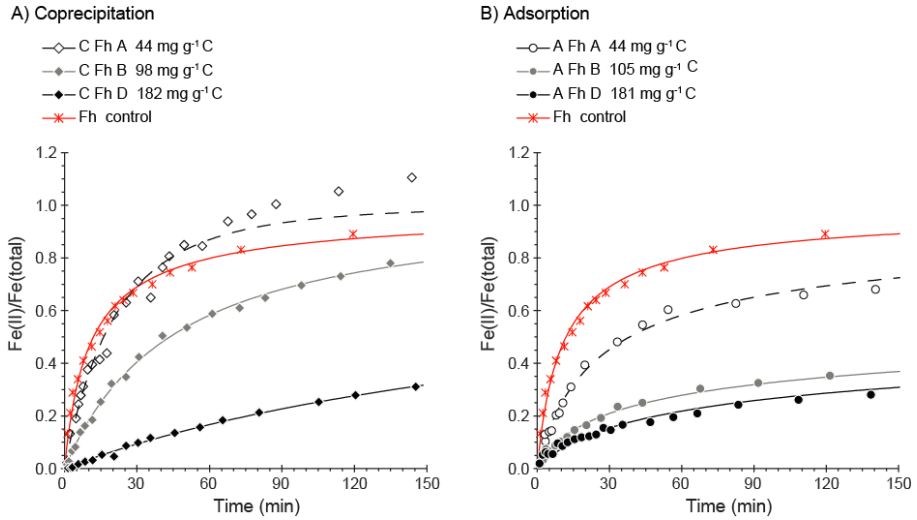

Fig. 4. Abiotic reduction with Na-dithionite: Fe(II) production (normalized to the total initial Fe in Fh) vs. time. Lines represent the model by Christoffersen and Christoffersen (1976). Note that the dissolved Fe(II) was estimated to be larger than the total Fe for sample CFhA, which is unreasonable.

BGD
11, 6039–6067, 2014